ACS Photonics

Letter

pubs.acs.org/journal/apchd5

Broadband Coherent Absorption in Chirped-Planar-Dielectric Cavities for 2D-Material-Based Photovoltaics and Photodetectors

Jiabao Zheng,*[,†,‡,§] Robert A. Barton,*[,†,∥] and Dirk Englund*[,§]

[‡]Department of Electrical Engineering and [∥]Energy Frontier Research Center, Columbia University, New York, New York 10027, United States

[§]Department of Electrical Engineering and Computer Science, Massachusetts Institute of Technology, Cambridge, Massachusetts 02139, United States

Supporting Information

ABSTRACT: Atomically thin materials such as graphene and transition metal dichalcogenides are being developed for a range of optoelectronic devices, but their applications are currently limited by low light absorption. Here, we describe a dielectric cavity design with chirped Bragg reflectors for broadband coherent absorption. The chirped cavity absorption is calculated by the transfer matrix method and optimized using the Nelder–Mead optimization protocol. We numerically demonstrate that with cavity enhancement, a monolayer MoS_2 photodetector absorbs as much as 33% of incident visible light over a 300 nm bandwidth, and the external quantum efficiency of an atomically thin monolayer graphene/monolayer MoS_2 solar cell can be enhanced 3.6 times to a predicted value of 7.09%. The proposed layered dielectric structures operate across a wide range of incident angles and could enable applications for atomically thin photodetectors or solar cells.

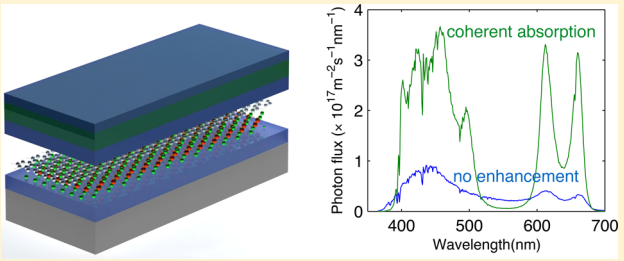

KEYWORDS: *optimization, graphene, transition metal dichalcogenides, absorption enhancement, chirped distributed Bragg reflector*

Atomically thin materials such as graphene or monolayer transition metal dichalcogenides exhibit unusually strong light-matter interaction relative to their thickness and offer significant advantages as potential light harvesters for optoelectronic devices.[1,2] However, light trapping techniques are required to overcome their low single-pass light absorption (2.3% for graphene across the visible spectrum and ∼10% at the band edge for MoS_2[3]). Graphene, because it has very large mobilities, can form the basis for ultrafast photodetectors[4] and high-speed optical modulators.[5] Owing to its large direct bandgap and corresponding low dark current, MoS_2 has comprised photodetectors with noise equivalent power as high as 1.8×10^{-15} W $Hz^{-1/2}$.[6] Atomically thin solar cells also seem viable. It has been theoretically predicted that a graphene/MoS_2 Schottky junction solar cell can achieve up to 1% power conversion efficiency, which corresponds to 1 to 3 orders of magnitude higher power densities than the best existing ultrathin solar cells.[7] Power conversion efficiencies as high as 18% are theoretically achievable for a bilayer phosphorene/MoS_2 heterojunction.[8] The advantages of 2D materials heterostructures for photovoltaics include flexibility, promising mobilities, atomically sharp interfaces, and diverse direct bandgaps spanning much of the solar spectrum.[9,10] The feasibility of optoelectronic devices[11−17] including solar cells[18,19] from 2D materials or vertical heterojunctions of several 2D material layers has been demonstrated experimentally.

Various light trapping techniques have been applied to enhance the optical absorption by thin-film materials.[20] Broadband coherent light absorbers have been studied for applications such as organic light-emitting diodes (OLEDs),[21] distributed feedback lasers,[22] photodetectors,[23] and solar cells.[24,25] However, studies of absorption enhancement for 2D materials have predominantly focused on narrow bandwidths. In the case of graphene, resonant absorption of 100% in the infrared region has been predicted utilizing the plasmonic response from patterned disks of graphene.[26] In the visible region, 100% absorption can be achieved in a narrow band by placing the graphene inside of a Fabry–Perot cavity[27] or on a photonic crystal.[28,29] Broadband absorption has been shown to be achievable for graphene within a narrow set of incident angles.[30,31] For photovoltaic applications and some photodetection applications, however, a robust absorption enhancement strategy must be effective when averaged over all incoming wavelengths and angles. For atomically thin materials such as monolayer MoS_2 or graphene, broadband coherent light trapping at normal incidence or averaged over incident angles has not yet been explored.

Here, we investigate broadband light absorption in atomically thin materials by incorporating them within layered stacks of dielectrics. We focus on a cavity that consists of a 2D material-on-spacer-on-reflector stack[32] with a chirped distributed Bragg

Received: April 5, 2014
Published: August 25, 2014

ACS Publications © 2014 American Chemical Society

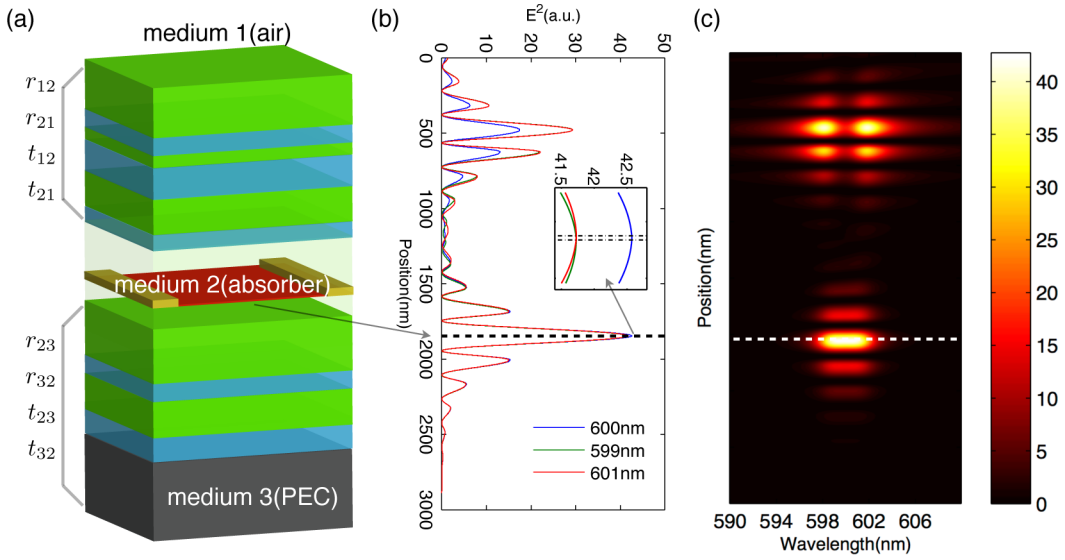

Figure 1. (a) General structure of the coherent broadband cavity explored in this work. (b) Electric field profile for an example cavity designed to maximize absorption over 599−601 nm is shown as a function of spatial position for incident light of wavelength 599, 600, and 601 nm. The absorption profile for this cavity is shown in Figure 2a. The inset is a magnification of the electric field intensity around the graphene. The black dashed lines indicate the placement of the graphene sheet. (c) Electric field vs space and wavelength (590−610 nm) for the same structure shown in (b); the white dashed line indicates the placement of the graphene sheet.

reflector (DBR) above the 2D material that adjusts the phase of the reflected light in a wavelength-dependent manner. Chirped DBRs have been previously investigated both in theory for dispersion compensation to generate ultra short laser pulses[33,34] and for their implementation in thin-film solar cells.[25,35] For example, absorption enhancement as high as 40% was obtained for organic photovoltaic devices using a structure similar to that proposed here.[25] Here, by casting the cavity design as an optimization problem and then using heuristic optimization techniques to achieve maximal absorption enhancement over a broad bandwidth, we find that adding a chirped dielectric cavity to a bilayer graphene/MoS_2 solar cell results in a 260% enhancement in external quantum efficiency (EQE), resulting in a maximum possible quantum efficiency exceeding 7%. For photodetection applications, we investigate the limits of broadband light trapping in this structure, showing that monolayer graphene can achieve almost 100% absorption over a 2 nm bandwidth around 600 nm (corresponding to a fractional bandwidth of $\Delta\omega/\omega_0 \sim 0.003$) or 8.5% absorption over a 360 nm bandwidth ($\Delta\omega/\omega_0 \sim 0.65$). An optimized cavity containing a single monolayer of MoS_2 can attain an average absorbance of 33.3% for above-bandgap photons. Unlike metallic structures for plasmon-mediated absorption enhancement,[20] the dielectric structures described here can have negligible parasitic absorption. The resulting absorption enhancement improves the viability of photodetectors and solar cells from 2D materials.

THEORETICAL CONSIDERATIONS

We consider a Gires-Tournois etalon-based layout in which the atomic absorber is sandwiched between a top and bottom mirror, as shown in Figure 1a. The cavity is terminated on one end with a perfect electric conductor (PEC). Using aperiodic dielectric stacks as cavity mirrors, we then tailor the complex reflectivity of the dielectric stacks to achieve critical coupling over a broad bandwidth. The cavity-enhanced absorption spectrum can, in this way, greatly exceed the Lorentzian spectrum of a typical cavity.

Considering the stack above and beneath the absorbing layer as the top and bottom mirrors, we denote the reflection (transmission) coefficient as r_{12} (t_{12}) for the top mirror and r_{23} (t_{23}) for the bottom mirror. The reflection coefficient of the whole cavity is then given by the transfer matrix method (TMM). By approximating the reflectivity of graphene as zero (see Supporting Information), ∼100% light absorption can be achieved analytically for this layout as long as the following two conditions on the top and bottom mirrors can be satisfied by, for instance, optimizing the layer thicknesses of the two dielectric stacks:

$$|r_{12}| = |t_g|^2 \tag{1a}$$

$$\phi_{r_{21}} + 2\phi_{t_g} + \phi_{r_{23}} = 2m\pi \tag{1b}$$

where m is an integer, t_g is the transmission coefficient of a suspended graphene sheet, and $\phi_{r_{21}}$, ϕ_{t_g}, and $\phi_{r_{23}}$ are the phases accumulated when light reflects from the top mirror, passes through the graphene, and reflects from the bottom mirror, respectively. The two conditions correspond to amplitude match and phase match. Should the two constraints be satisfied over a broad bandwidth, we can expect nearly 100% light absorption over this bandwidth. However, satisfying eq 1b would require broadband anomalous phase dispersion, which is nonphysical.[21]

We therefore seek to approach maximum possible broadband absorption by numerical optimization of the thicknesses of dielectrics in the stacks. Absorption is $A = 1 - R - T = 1 - R$ since no light is transmitted through the PEC. Therefore, maximizing the absorption is equivalent to minimizing the reflectivity, or in optimization form:

dx.doi.org/10.1021/ph500107b | ACS Photonics 2014, 1, 768−774

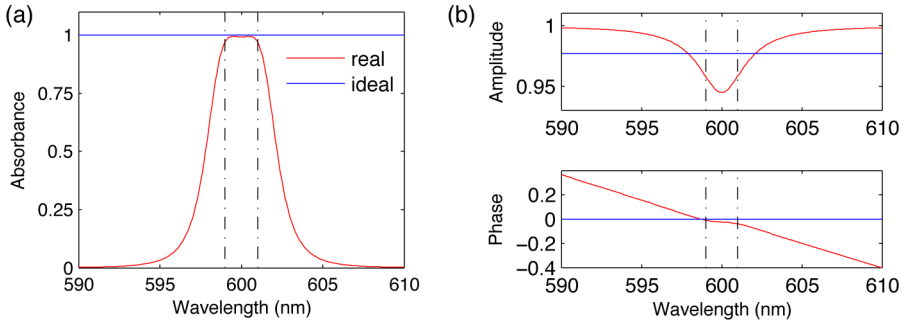

Figure 2. (a) Absorbance of as a function of wavelength for an optimized cavity which enables graphene to absorb ~100% of incoming light over a 2 nm bandwidth. (b) The plots show how this cavity satisfies the two matching conditions shown in eq 1. Top panel corresponds to eq 1a; the solid red line shows $|r_{12}|$, while the blue shows term $|t_g|^2$. Bottom panel corresponds to eq 1b; the line in red indicates the term $\phi_{r_{21}} + 2\phi_{t_g} + \phi_{r_{23}}$, while the blue line denotes the desired value of 0.

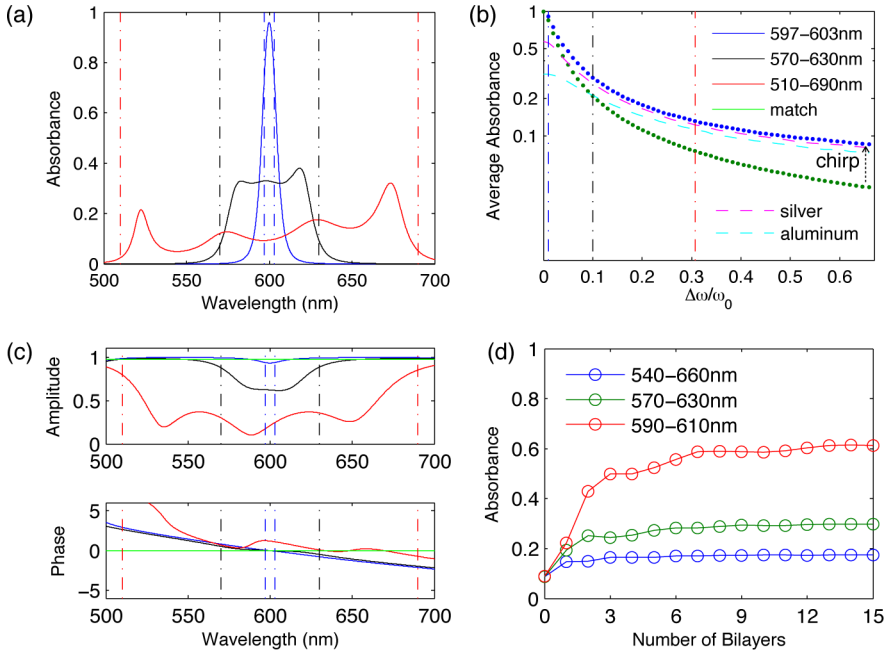

Figure 3. (a) Three optimized graphene cavities for different target bandwidth: Average absorbance is 90.7% for 597−603 nm (in blue), 29.4% for 570−630 nm (in black), and 13.2% for 510−690 nm (in red). (b) Log-scale absorbance averaged over target bandwidth as a function of normalized bandwidth. The dotted line in blue represents the optimized cavities, while the dotted green line shows a quarter-wave stack cavity reference, which corresponds to a cavity with critical coupling to 600 nm light. The blue/black/red dash-dotted lines correspond to three different target bandwidths indicated by the corresponding dash-dotted lines in (a). The dashed line in magenta/cyan denotes the average absorbance of the optimized cavities when they are terminated with silver/aluminum instead of a PEC. (c) The amplitude and phase match conditions are stated in eq 1. The green lines on the top and bottom panels show the right side of eq 1. The blue/black/red lines correspond to the three optimized cavities in (a), as shown in the legend in (b). (d) For different target bandwidths, average absorption as a function of the number of bilayers in the top mirror.

$$\underset{t\in R^n}{\text{minimize}} \; \frac{\int_{\lambda_1}^{\lambda_2} R(\lambda, t) w(\lambda) \mathrm{d}\lambda}{\int_{\lambda_1}^{\lambda_2} w(\lambda) \mathrm{d}\lambda}$$

$$\text{subject to } t_i \geq 0,\ i = 1, \ldots, n \qquad (2)$$

where n is the total number of dielectric layers and t_i is the thickness of the ith layer. The objective function, which is the cavity intensity reflection coefficient as a function of all thickness variables, can be calculated using TMM. The optimization problem is multiextremal and nonlinear, with many parameters and a large search space, as is common for such problems. Applicable numerical algorithms include genetic algorithms, dynamic programming, simulated annealing, and Monte Carlo techniques.[36] We tested various heuristic search techniques in MATLAB and found the best performance for genetic algorithms and a Nelder−Mead simplex method, and also good agreement between TMM and RCWA (rigorous coupled-wave analysis) using Rsoft (see Supporting Information). These optimizations are performed for different values of λ_1,λ_2, depending on the application. The weighting function $w(\lambda)$ in eq 2 equals the solar flux spectrum for solar cell optimization, while for photodetection applications $w(\lambda) = 1$.

RESULTS AND DISCUSSION

Coherent Absorption for Photodetectors. To investigate the limits of absorption enhancement using this approach, we optimize absorption over different bandwidths for graphene, for which we can compare our results to the baseline value of 2.3% broadband absorption. First, we aim for

dx.doi.org/10.1021/ph500107b | ACS Photonics 2014, 1, 768−774

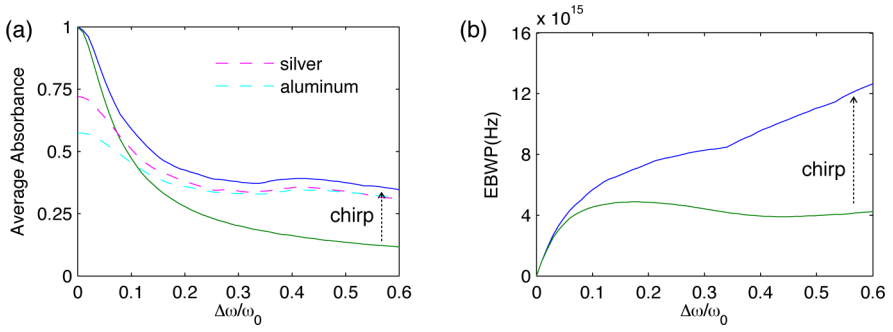

Figure 4. (a) Average absorbance and (b) EBWP over different target bandwidths (center wavelength 520 nm) for monolayer MoS_2 in different optimized cavities. Solid lines in blue (green) indicate the optimal (naive) case. In (a), the dashed line in magenta/cyan denotes the average absorbance of the optimized cavities when they are terminated with silver/aluminum instead of a PEC.

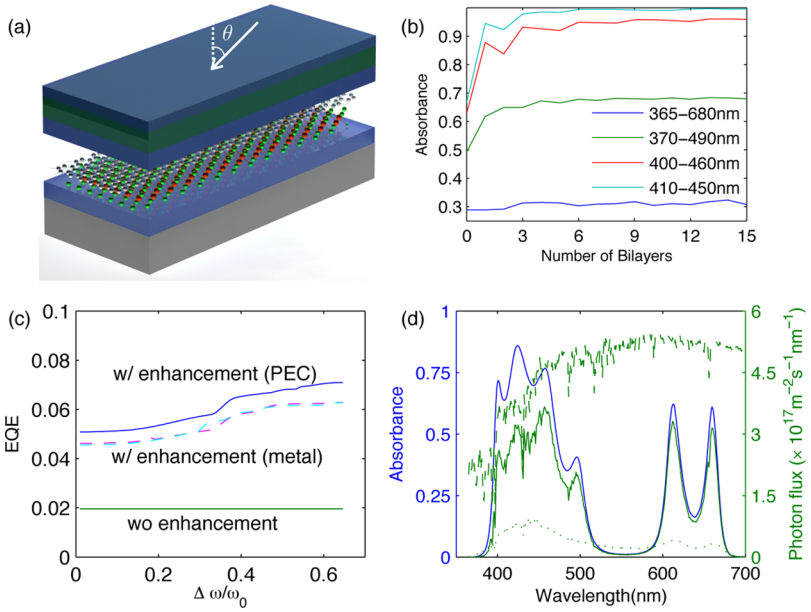

Figure 5. (a) Schematic structure of a solar cell made of a single layer of graphene on a single layer of MoS_2. (b) Absorbance over different bandwidths as a function of number of layer pairs in the top mirror. The bottom mirror is a dielectric spacer followed by a PEC. (c) EQE of cavities with graphene/MoS_2 optimized over different target bandwidths, with center wavelength at 520 nm (blue line). The highest EQE is 7.09%, corresponding to the cavity optimized over 366.6−673.4 nm. The green line indicates the EQE of graphene/MoS_2 without a cavity, which is 1.96%, assuming the internal quantum efficiency is 1. The dashed line in magenta/cyan denotes the EQE of the optimized cavities when they are terminated with silver/aluminum instead of a PEC. (d) Absorbance (left axis) and absorbed photon flux (right axis) as a function of wavelength. This corresponds to the cavity that has the highest EQE in (c). The blue solid line denotes the absorbance of this cavity for uniformly distributed light. The dashed green line shows the incident solar photon flux, while the solid green line is the photon flux absorbed by the optimized cavity, and the dotted green line is the absorbed photon flux without a cavity.

nearly 100% absorption over a small bandwidth. As shown in Figure 2, the optimum cavity design achieved 98.9% absorbance over a 2 nm bandwidth for a single layer of graphene. The simulated phase and reflection amplitudes show good agreement with eq 1 (shown in Figure 2b), indicating that nearly 100% destructive interference was achieved over 599−601 nm bandwidth. This optimized cavity has 12 pairs of alternating dielectrics in the top mirror and 9 bilayers in the bottom mirror, with layer thicknesses ranging from 53 to 155 nm. The electric field of this optimized cavity is shown in Figure 1b for 599, 600, and 601 nm light. Figure 1c gives the electric field as a function of both space and wavelength, which shows that multiple modes give rise to the broadband absorption.

As the target bandwidth increases, we find that replacing the bottom mirror with a spacer consisting of a single dielectric layer results in negligible absorption loss. For simplicity, therefore, the remainder of the paper focuses on a stack consisting of a top chirped mirror and an atomically thin absorber followed by a spacer and a reflector. In Figure 3a, we obtain three optimal cavities for three different normalized target bandwidths with center wavelength 600 nm. The average absorbance over the target range decreases as a function of normalized target bandwidth (Figure 3b, blue dotted line). However, the average broadband absorbance is superior to that obtained by a "naive" quarter-wave stack cavity optimized for a single wavelength, as calculated analytically (Figure 3b, green dotted line).[37] As we increase the target bandwidth, the average absorbance of the optimized graphene cavities decreases, since it becomes difficult to satisfy eq 1, as shown in Figure 3c. However, for a 420−780 nm bandwidth, the average absorbance of the optimized cavity is 8.5%, nearly three times greater than the corresponding value of 2.9% for the quarter-

dx.doi.org/10.1021/ph500107b | ACS Photonics 2014, 1, 768−774

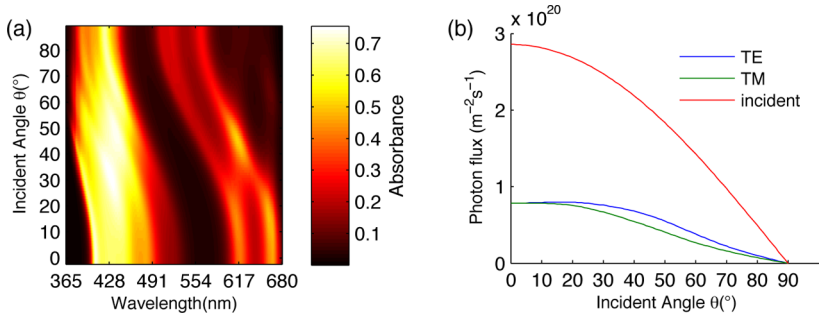

Figure 6. (a) Absorbance of an optimal cavity vs wavelength and incident angle, bandwidth 365−680 nm. The maximum absorbance sits at (λ = 430.5 nm, θ = 33°), indicating that the optimized cavity has the strongest absorption (power absorption of 75.5%) coefficient at θ = 33° even though the intensity of angled incident light is weighted lower than that of normal incidence light ($I \sim \cos\theta$). (b) Performance of the optimized cavity for different polarization as a function of angle. The blue (green) solid line indicates the absorbed photon flux when the incident solar power is entirely TE (TM).

wave cavity. Furthermore, the impact of replacing the PEC with a realistic metal mirror is determined and shown by the dashed lines in Figure 3b. In the broadband case, the average absorbance is ∼8.0% when the cavity is followed by silver instead of a PEC (dashed line in magenta), while the broadband average absorbance is ∼7.2% for an aluminum mirror (dashed line in cyan). The minor difference (8.0% in the case of silver compared to 8.5% in the PEC case) between using a PEC for our structure and using a metal mirror justifies the viability of using a PEC instead of a metal material in our simulation. As shown in Figure 3d, average absorbance over different bandwidths depends on the number of layer pairs on top mirror, indicating the cost-benefit trade-off involved in fabricating cavities with many dielectric layers.

In Figure 4 we show results for cavities containing only monolayer MoS_2 as the photoactive material, with the intent of enhancing MoS_2 absorption for photodetection.[6] We assume a center wavelength of 520 nm. Figure 4a shows that the average absorbance of the optimized chirped-DBR cavity is markedly superior to that of the quarter-wave stack cavity reference, with a maximum average absorption of 33.3% attained for a 370−670 nm target bandwidth, compared to 11.1% over the same bandwidth for the reference cavity. To analyze this improvement, we plot in Figure 4b the enhancement-bandwidth product (EBWP). The EBWP is the product of the absorption enhancement and the target bandwidth, which is proportional to total number of photons absorbed assuming a flat spectral distribution of incoming light. With a "naive" cavity, the EBWP stays roughly constant as our target bandwidth increases, but for the optimized cavity, the EBWP increases dramatically with target bandwidth. For narrow target bandwidths, therefore, the chirped DBR enhances absorption no better than the naive cavity, but as bandwidth increases, chirping the cavity produces much stronger absorption.

Coherent Absorption for 2D-Material Solar Photovoltaics. Next, we analyze the efficiencies of solar cells made from 2D materials that benefit from coherent broadband light trapping. An example device structure made from a graphene/MoS_2 bilayer, as proposed by Bernardi et al.,[7] is shown in Figure 5a. For this section, we use EQE over the full solar spectrum (280−4000 nm) as the figure of merit, assuming that each photon absorbed by the MoS_2 generates one electron−hole pair. We use Global Tilt data from ASTMG173−03 Reference Spectra as the weighting function $w(\lambda)$ in eq 2.

The optimized results are shown in Figure 5c,d. With no photonic enhancement, the absorption of the MoS_2 in the graphene/MoS_2 bilayer is 1.96%. With the cavity optimized over 366.6−673.4 nm (see Methods), we predict an optimal weighted average absorption of 7.09% over 280−4000 nm, representing a 260% improvement in EQE. We also investigate the absorbance as a function of the number of bilayers in the top mirror in Figure 5b. The results show diminishing returns as the number of layers increases, suggesting that only several dielectric layers are necessary to make a near-optimal top mirror. In particular, we found that by removing the top mirror and optimizing only the thickness of the spacer (optimal thickness: 71.82 nm for the low index material n_L = 1.5),[38] the average absorbance of 365−680 nm light increases from 8.88% single pass absorption to 28.85%, while with an optimal top mirror the absorbance over the same range increases to 32.35%.

For solar cell applications, it is also important to address the angular dependence of absorption enhancement. Using Lambert's cosine law (solar intensity $I \sim \cos\theta$) for angular dependence, assuming that the TE/TM mode are equally distributed in incident solar power, and using a target bandwidth of 365−680 nm, we found that an optimal graphene/MoS_2 solar cell can absorb 26.72% of incident solar photons (compared to 30.71% absorption for this configuration for normal incidence light only). The polarization dependence in Figure 6b shows that this optimized cavity favors TE polarization over TM mode polarization, perhaps because TM polarized light is restricted by the waveguide mode of the layer dielectric structure.

Fabrication of 1D photonic crystal cavities incorporating 2D materials is possible using various techniques, including chemical vapor deposition (CVD) or spin-coating. Recent work on MoS_2 synthesis has demonstrated growth in large areas directly on SiO_2.[39] Therefore, fabrication of the proposed solar cell could start with the chirped DBR terminating with SiO_2, followed by CVD growth of MoS_2 directly on top of the oxide, and finishing with lamination of the graphene[40] followed by evaporation of contacts, a spacer and reflector such as a highly conductive metallic mirror. Using this method, integration difficulties should be minimized since the DBR can be entirely fabricated before integration with the 2D material.

For photonic applications of 2D materials, enhancing light-matter interaction will be of crucial importance. In this work, we demonstrated a simple layered structure that can greatly enhance broadband absorption for 2D materials. The simulations indicate a large broadband absorption enhancement produced in graphene for light at normal incidence, achieving 8.5% absorption in graphene over a 360 nm bandwidth. With

dx.doi.org/10.1021/ph500107b | ACS Photonics 2014, 1, 768−774

respect to applications, we demonstrate that a single layer of MoS_2 in such a cavity can absorb 33.3% of above-bandgap light, and we predict over 7% external quantum efficiency for a bilayer graphene/MoS_2 solar cell. Our layered structures are relatively simple to fabricate, and the analysis and optimization approach is generalizable to other 2D materials. Our results suggest that 2D materials−based optoelectronic devices incorporating additional layers of material to enhance absorption will be capable of achieving quantum efficiencies comparable to those of traditional photovoltaic materials.

METHODS

For dielectric mirrors, we use materials with indices $n_H = 2.5$ and $n_L = 1.5$, close to the values for TiO_2 and SiO_2, respectively. For graphene, we use the effective complex refractive index in the visible range[41]

$$n_g = 3.0 - i\frac{C}{3}\lambda \tag{3}$$

where $C = 5.446\ \mu m^{-1}$ and a graphene thickness $t = 0.34$ nm is assumed. As a test, an absorption of 2.27% is obtained by setting all the thickness variables to zero and changing the PEC material to air, indicating that graphene absorbs 2.27% of light for a single pass, which is close to the exact value $\pi\alpha = 2.3\%$[42] in the linear dispersion regime.

For monolayer MoS_2, we use a thickness $t = 0.65$ nm and an experimentally measured refractive index for wavelengths ranging from 365 to 680 nm[43] (there is no absorption above the MoS_2 bandgap at ∼680 nm). For MoS_2 in air, the TMM indicates an average absorbance of 8.91% from 365 to 680 nm. For solar cell simulations, the refractive index of MoS_2 is matched to the solar spectrum using nearest interpolation. We also note that for a suspended bilayer of graphene/MoS_2, the average absorbance is 10.74%. However, for our hypothetical graphene/MoS_2 solar cell, we set the graphene absorbance to zero since electron−hole pairs generated in the graphene are expected to recombine before they can be extracted.

ASSOCIATED CONTENT

Supporting Information

Exact derivation of eq 1 from TMM, the numerical demonstration of the related approximation, convergence with other optimization techniques, and the verification results by RCWA. This material is available free of charge via the Internet at http://pubs.acs.org.

AUTHOR INFORMATION

Corresponding Authors

*E-mail: jz2466@columbia.edu.
*E-mail: rab375@cornell.edu.
*E-mail: englund@mit.edu.

Author Contributions

†These authors contributed equally to this work (J.Z. and R.A.B.).

Notes

The authors declare no competing financial interest.

ACKNOWLEDGMENTS

The authors thank Yilei Li for providing absorption spectra and Richard Grote, Cheng-Chia Tsai, and Paul George for helpful discussions. This material is primarily based on work supported as part of the Center for Re-Defining Photovoltaic Efficiency Through Molecule Scale Control, an Energy Frontier Research Center funded by the U.S. Department of Energy, Office of Science, Office of Basic Energy Sciences under Award Number DE-SC0001085. This work is also supported by a matching grant from the Empire State Development's Division of Science, Technology and Innovation (NYSTAR), as well as by the New York State Energy Research Development Authority (NYSERDA).

REFERENCES

(1) Bonaccorso, F.; Sun, Z.; Hasan, T.; Ferrari, A. C. Graphene photonics and optoelectronics. *Nat. Photonics* **2010**, *4*, 611−622.
(2) Wang, Q. H.; Kalantar-Zadeh, K.; Kis, A.; Coleman, J. N.; Strano, M. S. Electronics and optoelectronics of two-dimensional transition metal dichalcogenides. *Nat. Nanotechnol.* **2012**, *7*, 699−712.
(3) Mak, K. F.; Lee, C.; Hone, J.; Shan, J.; Heinz, T. F. Atomically thin MoS_2: A new direct-gap semiconductor. *Phys. Rev. Lett.* **2010**, *105*, 136805.
(4) Gan, X.; Shiue, R.-J.; Gao, Y.; Meric, I.; Heinz, T. F.; Shepard, K.; Hone, J.; Assefa, S.; Englund, D. Chip-integrated ultrafast graphene photodetector with high responsivity. *Nat. Photonics* **2013**, *7*, 883−887.
(5) Liu, M.; Yin, X.; Ulin-Avila, E.; Geng, B.; Zentgraf, T.; Ju, L.; Wang, F.; Zhang, X. A graphene-based broadband optical modulator. *Nature* **2011**, *474*, 64−67.
(6) Lopez-Sanchez, O.; Lembke, D.; Kayci, M.; Radenovic, A.; Kis, A. Ultrasensitive photodetectors based on monolayer MoS_2. *Nat. Nanotechnol.* **2013**, *8*, 497−501.
(7) Bernardi, M.; Palummo, M.; Grossman, J. C. Extraordinary sunlight absorption and one nanometer thick photovoltaics using two-dimensional monolayer materials. *Nano Lett.* **2013**, *13*, 3664−3670.
(8) Dai, J.; Zeng, X. C. Bilayer phosphorene: Effect of stacking order on bandgap and its potential applications in thin-film solar cells. *J. Phys. Chem. Lett.* **2014**, *5*, 1289−1293.
(9) Wang, Q. H.; Kalantar-Zadeh, K.; Kis, A.; Coleman, J. N.; Strano, M. S. Electronics and optoelectronics of two-dimensional transition metal dichalcogenides. *Nat. Nanotechnol.* **2012**, *7*, 699−712.
(10) Jariwala, D.; Sangwan, V. K.; Lauhon, L. J.; Marks, T. J.; Hersam, M. C. Emerging device applications for semiconducting two-dimensional transition metal dichalcogenides. *ACS Nano* **2014**, *8*, 1102−1120.
(11) Baugher, B. W.; Churchill, H. O.; Yang, Y.; Jarillo-Herrero, P. Optoelectronic devices based on electrically tunable p-n diodes in a monolayer dichalcogenide. *Nat. Nanotechnol.* **2014**, *9*, 262−267.
(12) Pospischil, A.; Furchi, M. M.; Mueller, T. Solar-energy conversion and light emission in an atomic monolayer p-n diode. *Nat. Nanotechnol.* **2014**, *9*, 257−261.
(13) Lee, C.-H.; Lee, G.-H.; van der Zande, A. M.; Chen, W.; Li, Y.; Han, M.; Cui, X.; Arefe, G.; Nuckolls, C.; Heinz, T. F.; Guo, J.; Hone, J.; Kim, P. Atomically thin p−n junctions with van der Waals heterointerfaces. *arXiv preprint* **2014**, DOI: arXiv:1403.3062.
(14) Furchi, M. M.; Pospischil, A.; Libisch, F.; Burgdörfer, J.; Mueller, T. Photovoltaic effect in an electrically tunable van der Waals heterojunction. *arXiv preprint* **2014**, DOI: arXiv:1403.2652.
(15) Britnell, L.; Ribeiro, R. M.; Eckmann, A.; Jalil, R.; Belle, B. D.; Mishchenko, A.; Kim, Y.-J.; Gorbachev, R. V.; Georgiou, T.; Morozov, S. V.; Grigorenko, A. N.; Geim, A. K.; Casiraghi, C.; Neto, A. H. C.; Novoselov, K. S. Strong light-matter interactions in heterostructures of atomically thin films. *Science* **2013**, *340*, 1311−1314.
(16) Yu, W. J.; Liu, Y.; Zhou, H.; Yin, A.; Li, Z.; Huang, Y.; Duan, X. Highly efficient gate-tunable photocurrent generation in vertical heterostructures of layered materials. *Nat. Nanotechnol.* **2013**, *8*, 952−958.
(17) Ross, J. S.; Klement, P.; Jones, A. M.; Ghimire, N. J.; Yan, J.; G, M.; Taniguchi, T.; Watanabe, K.; Kitamura, K.; Yao, W.; Cobden, D. H.; Xu, X. Electrically tunable excitonic light-emitting diodes based on monolayer WSe_2 p−n junctions. *Nat. Nanotechnol.* **2014**, *9*, 268−272.

(18) Lopez-Sanchez, O.; Alarcon Llado, E.; Koman, V.; Fontcuberta i Morral, A.; Radenovic, A.; Kis, A. Light generation and harvesting in a van der Waals heterostructure. *ACS Nano* **2014**, *8*, 3042−3048.
(19) Miao, X.; Tongay, S.; Petterson, M. K.; Berke, K.; Rinzler, A. G.; Appleton, B. R.; Hebard, A. F. High efficiency graphene solar cells by chemical doping. *Nano Lett.* **2012**, *12*, 2745−2750.
(20) Basu Mallick, S.; Sergeant, N. P.; Agrawal, M.; Lee, J.-Y.; Peumans, P. Coherent light trapping in thin-film photovoltaics. *MRS Bull.* **2011**, *36*, 453−460.
(21) Agrawal, M.; Peumans, P. Design of non-periodic dielectric stacks for tailoring the emission of organic lighting-emitting diodes. *Opt. Express* **2007**, *15*, 9715−9721.
(22) Das, B. K.; Ricken, R.; Quiring, V.; Suche, H.; Sohler, W. Distributed feedback-distributed Bragg reflector coupled cavity laser with a Ti:(Fe:)Er:$LiNbO_3$ waveguide. *Opt. Lett.* **2004**, *29*, 165−167.
(23) Ferreira, A.; Peres, N. M. R.; Ribeiro, R. M.; Stauber, T. Graphene-based photodetector with two cavities. *Phys. Rev. B* **2012**, *85*, 115438.
(24) Raman, A.; Yu, Z.; Fan, S. Dielectric nanostructures for broadband light trapping in organic solar cells. *Opt. Express* **2011**, *19*, 19015−19026.
(25) Agrawal, M.; Peumans, P. Broadband optical absorption enhancement through coherent light trapping in thin-film photovoltaic cells. *Opt. Express* **2008**, *16*, 5385−5396.
(26) Thongrattanasiri, S.; Koppens, F. H. L.; García de Abajo, F. J. Complete optical absorption in periodically patterned graphene. *Phys. Rev. Lett.* **2012**, *108*, 047401.
(27) Furchi, M.; Urich, A.; Pospischil, A.; Lilley, G.; Unterrainer, K.; Detz, H.; Klang, P.; Andrews, A. M.; Schrenk, W.; Strasser, G.; Mueller, T. Microcavity-integrated graphene photodetector. *Nano Lett.* **2012**, *12*, 2773−2777.
(28) Piper, J. R.; Fan, S. Total absorption in a graphene monolayer in the optical regime by critical coupling with a photonic crystal guided resonance. *ACS Photonics* **2014**, *1*, 347−353.
(29) Shiue, R.-J.; Gan, X.; Gao, Y.; Li, L.; Yao, X.; Szep, A.; Walker, D.; Hone, J.; Englund, D. Enhanced photodetection in graphene-integrated photonic crystal cavity. *Appl. Phys. Lett.* **2013**, *103*, 241109.
(30) Pirruccio, G.; Martín Moreno, L.; Lozano, G.; Gómez Rivas, J. Coherent and broadband enhanced optical absorption in graphene. *ACS Nano* **2013**, *7*, 4810−4817.
(31) Zhao, W.; Shi, K.; Lu, Z. Greatly enhanced ultrabroadband light absorption by monolayer graphene. *Opt. Lett.* **2013**, *38*, 4342−4345.
(32) Blake, P.; Hill, E. W.; Castro Neto, A. H.; Novoselov, K. S.; Jiang, D.; Yang, R.; Booth, T. J.; Geim, A. K. Making graphene visible. *Appl. Phys. Lett.* **2007**, *91*, 063124.
(33) Kärtner, F. X.; Matuschek, N.; Schibli, T.; Keller, U.; Haus, H. A.; Heine, C.; Morf, R.; Scheuer, V.; Tilsch, M.; Tschudi, T. Design and fabrication of double-chirped mirrors. *Opt. Lett.* **1997**, *22*, 831−833.
(34) Szipocs, R.; Khzi-Kis, A. Theory and design of chirped dielectric laser mirrors. *Appl. Phys. B: Lasers Opt.* **1997**, *65*, 115−135.
(35) Kuzma-Filipek, I. J.; Duerinckx, F.; Van Kerschaver, E.; Van Nieuwenhuysen, K.; Beaucarne, G.; Poortmans, J. Chirped porous silicon reflectors for thin-film epitaxial silicon solar cells. *J. Appl. Phys.* **2008**, *104*, 073529.
(36) Weile, D. S.; Michielssen, E. Genetic algorithm optimization applied to electromagnetics: a review. *IEEE Trans. Antennas Propag.* **1997**, *45*, 343−353.
(37) Kishino, K.; Unlu, M.; Chyi, J.-I.; Reed, J.; Arsenault, L.; Morkoc, H. Resonant cavity-enhanced (RCE) photodetectors. *IEEE J. Quantum Electron.* **1991**, *27*, 2025−2034.
(38) Liu, J.-T.; Wang, T.-B.; Li, X.-J.; Liu, N.-H. Enhanced absorption of monolayer MoS2 with resonant back reflector. *J. Appl. Phys.* **2014**, *115*, 193511.
(39) van der Zande, A. M.; Huang, P. Y.; Chenet, D. A.; Berkelbach, T. C.; You, Y.; Lee, G.-H.; Heinz, T. F.; Reichman, D. R.; Muller, D. A.; Hone, J. C. Grains and grain boundaries in highly crystalline monolayer molybdenum disulphide. *Nat. Mater.* **2013**, *12*, 554−561.
(40) Bae, S.; et al. Roll-to-roll production of 30-in. graphene films for transparent electrodes. *Nat. Nanotechnol.* **2010**, *5*, 574−578.
(41) Bruna, M.; Borini, S. Optical constants of graphene layers in the visible range. *Appl. Phys. Lett.* **2009**, *94*, 031901.
(42) Nair, R. R.; Blake, P.; Grigorenko, A. N.; Novoselov, K. S.; Booth, T. J.; Stauber, T.; Peres, N. M. R.; Geim, A. K. Fine Structure Constant Defines Visual Transparency of Graphene. *Science* **2008**, *320*, 1308.
(43) Li, Y.; Chernikov, A.; Zhang, X.; Rigosi, A.; Hill, H.; van der Zande, A.; Chenet, D. A.; Shih, E.-M.; Hone, J.; Heinz, T. F. Measurement of the in-plane optical dielectric functions of monolayer transition metal dichalcogenides: MoS_2, $MoSe_2$, WS_2, and WSe_2. Unpublished.